Towards an in-plane methodology to track breast lesions by using mammograms and patient-specific finite element simulations

Andrés Lapuebla-Ferri [1]

José Cegoñino-Banzo [2]

Antonio-José Jiménez-Mocholí [1]

Amaya Pérez del Palomar [2] **(corresponding author)**

amaya@unizar.es

[1] Department of Continuum Mechanics and Theory of Structures.

School of Industrial Engineering.

Universitat Politècnica de València.

Camino de Vera s/n. E-46022 Valencia (Spain).

[2] GBM – Biomaterials Group.

Aragón Institute of Engineering Research (I3A).

Mechanical Engineering Department.

Universidad de Zaragoza.

María de Luna, s/n. E-50018 Zaragoza (Spain).

Phone: (+34) 976 76 28 72.

Abstract

In breast cancer screening or diagnosis, it is usual to combine different images in order to locate a lesion as accurately as possible. These images are generated by using a single or several imaging techniques. As X-ray based mammography is used widespread, a breast lesion is located in the same plane of the image (mammogram), but tracking of a breast lesion across mammograms corresponding to different views is a daring task for medical physicians. According to this, simulation tools and methodologies that use patient-specific numerical models can facilitate the task of fusing information from different images. Additionally, these tools need to be as straightforward as possible to facilitate its translation to the clinical area.

This paper presents a patient-specific, finite element (FE) based and semi-automated simulation methodology to track breast lesions across mammograms. A realistic, three-dimensional, computer model of a patient's breast was generated from magnetic resonance imaging (MRI) to simulate mammographic compressions in cranio-caudal (CC, head-to-toe) and medio-lateral oblique (MLO, shoulder-to-opposite hip) directions. For each compression being simulated, a *virtual mammogram* was obtained and posteriorly superimposed to the corresponding real mammogram, by sharing the nipple as a common feature. Two-dimensional rigid-body transformations were applied, and the error distance measured between the centroids of the tumor previously located on each image was 3.84 mm and 2.41 mm for CC and MLO compression, respectively. Considering that the scope of this work is to conceive a methodology translatable to the clinical practice, the results indicate that it could be helpful to support tracking of breast lesions.

1. Introduction

Breast cancer is the leading cause of cancer deaths among western world women[1]. Prevention policies have led to screening programs that allow early detection and subsequent therapy application, thus permitting a better prognosis (Jemal *et al* 2010). X-ray-based mammography is the gold standard in breast screening and cancer diagnosis due to its good specificity and low cost. If suspicious masses are found, MRI is also commonly used since it has a higher sensitivity but a higher cost and a lower specificity. It is accepted that combination of both techniques provides a more reliable diagnosis (Malur *et al* 2001) (Drukker *et al* 2005).

The task of fusing information from different images is known as *image registration*. Its main goal is to obtain the transformation that relates the corresponding regions found in similar images (Guo *et al* 2006) – i. e, mammograms – or to calculate the correspondence between points in an image *I* and those in a fixed reference image, or the physical space of an intervention *R* (Hipwell *et al* 2016). Tracking lesions across mammograms has to deal with the high deformability of the breast due to changes in patient position or to forces exerted during the clinical setting. In a mammography, the patient is standing and each breast is highly compressed between two plates and, from this process, two mammograms are obtained, usually in CC and MLO directions. However, in MRI, the patient lies prone with her breasts pending down and thus subjected to gravity action. Hence, the high deformability of the breast makes the tumor tracking between mammograms a challenging task, which is intimately related to the problem of predicting breast deformations.

In the last decade, remarkable works have employed FE models to predict breast deformation under gravity action (Rajagopal *et al* 2008) (Kuhlmann *et al* 2013), when a patient change her position from supine to upright (Pérez del Palomar *et al*, 2008) (Han *et al* 2014) (Khatam *et al* 2015), or during clinical settings, such as needle biopsy (Azar *et al* 2001) or mammography (Chung *et al* 2008) (Tanner *et al* 2011) (Han *et al* 2012). To a greater or lesser extent, the authors have related these works with inter-modal (mammogram-to-mammogram) or intra-modal (i.e.,

---

[1] World Health Organization. URL: http://www.who.int. Accessed May 13, 2017.

mammogram-to-MRI) medical image registration. In addition, other works can be found in which FE simulations are used specifically within an image registration framework. The first works were carried out by Samani *et al* (2000). A CC-mammographic compression was simulated in order to fuse data from X-Ray to MRI images. The mechanics of a contact problem and the nonlinear properties of the tissues involved were considered. However, the FE model was unrealistic, and the degree of compression of the breast during simulation was too low compared to the level usually reached on a clinical setting (Samani *et al* 2001). Besides, it was not specified how the model could support data fusion.

Schnabel *et al* (2003) presented a FE-based methodology to validate nonrigid image registration methods, but they considered a linear elastic response for the tissues involved. Ruiter *et al* (2006) developed a FE-based methodology to register MRI and mammograms. In this work, a mean registration error of 4.3 mm was obtained, a good result in the field of tumor localization. Nevertheless, the contact mechanics of the model were not stated sufficiently. Pathmanathan *et al* (2008) simulated breast compressions to match a point in a CC mammogram with the corresponding region in a MLO mammogram. Besides, it was computed the reference, stress-free state of the breast (i.e, without taking into account gravity action) as it was done previously by Rajagopal *et al* (2008). Though the results were promising, the model lacked of clinical validation. Furthermore, the proposed methodology was judged difficult to put into practice. Chung *et al* (2008) presented a FE-based methodology which was intended to trace the position of a tumor during a mammographic compression. Errors lesser than 5.0 mm in the location of markers were measured, but the model was little realistic. Lee *et al* (2013) presented a simulation framework to perform mammograms-MRI registration. CC and MLO compressions were carried out to the breast models, but those were manually generated. In addition, the tumor localization errors were too high, ranging from 7.5 mm to 33.0 mm.

In some works, the authors use FE simulations within an intensity-based registration framework to optimize the parameters involved in the analysis, but they have some shortcomings. Hopp *et al* (2013) only considered CC mammograms, while in the clinical setting is prescriptive to compress the breast in two directions. This was corrected by Mertzanidou *et al* (2014) but the mean registration error was 11.6 mm and 11.0 mm for CC and MLO mammograms, respectively. Solves-Llorens *et al* (2014) developed a software application to register automatically X-ray mammograms and MRI, but the geometry of the FE model is believed to be excessively simplistic.

Finally, there can be found some registration frameworks that are scarce in the literature, but they are interesting in the sense that they can open new research ways to investigate methodologies to track breast lesions. Ong *et al* (2010) used FE simulations within a surface-based non-rigid registration framework that provided good results.

The state-of-art of breast simulation evidences that the question of how to track breast tumors across different medical images is still not solved in a practical way. The importance of this issue is that an adequate framework to track tumors could allow a better diagnosis or even support surgery planning to remove breast lesions. Nevertheless, such a method should meet the requirements of individualization to a particular patient, accuracy in a sufficient degree and potential translatability to the clinical area. In fact, although many of the previously cited works are able to fulfill the first one with enough accuracy, their practical applicability is believed to be difficult.

In this paper, the authors propose a methodology to track a breast lesion in plane previously detected in both X-ray mammograms and MRI. A realistic, patient-based and large deformable FE model of the breast is generated and used to simulate breast compressions as it was done during mammography. Among other assumptions, the number of parameters to define the

material constitutive models was reduced with respect to previous works with the aim of obtaining an accurate but faster methodology that could be applied to clinical practice.

2. Methods

The case of study employed in this work corresponded to a 56-year-old European female who was diagnosed of a nodule attached to the left inferior quadrant of the left breast by means of X-ray mammography (Konica Minolta, 4014 x 5416 pixel x pixel resolution, 0.04375-mm^2 pixel size) (Figures 1a, 1b). A written informed consent was obtained to use the medical images in this work.

2.1. Model generation

Following intravenous gadolinium intake to enhance contrast, a MRI scan was performed (Siemens Symphony Maestro 1.5 T scanner, 512 x 320-pixel resolution, 0.664-mm^2 pixel size, 1.4-mm slice thickness) and 352 axial, sagittal and coronal images were taken with a fat suppression sequence (Figure 1c, 1d, 1e).

(a)   (b)

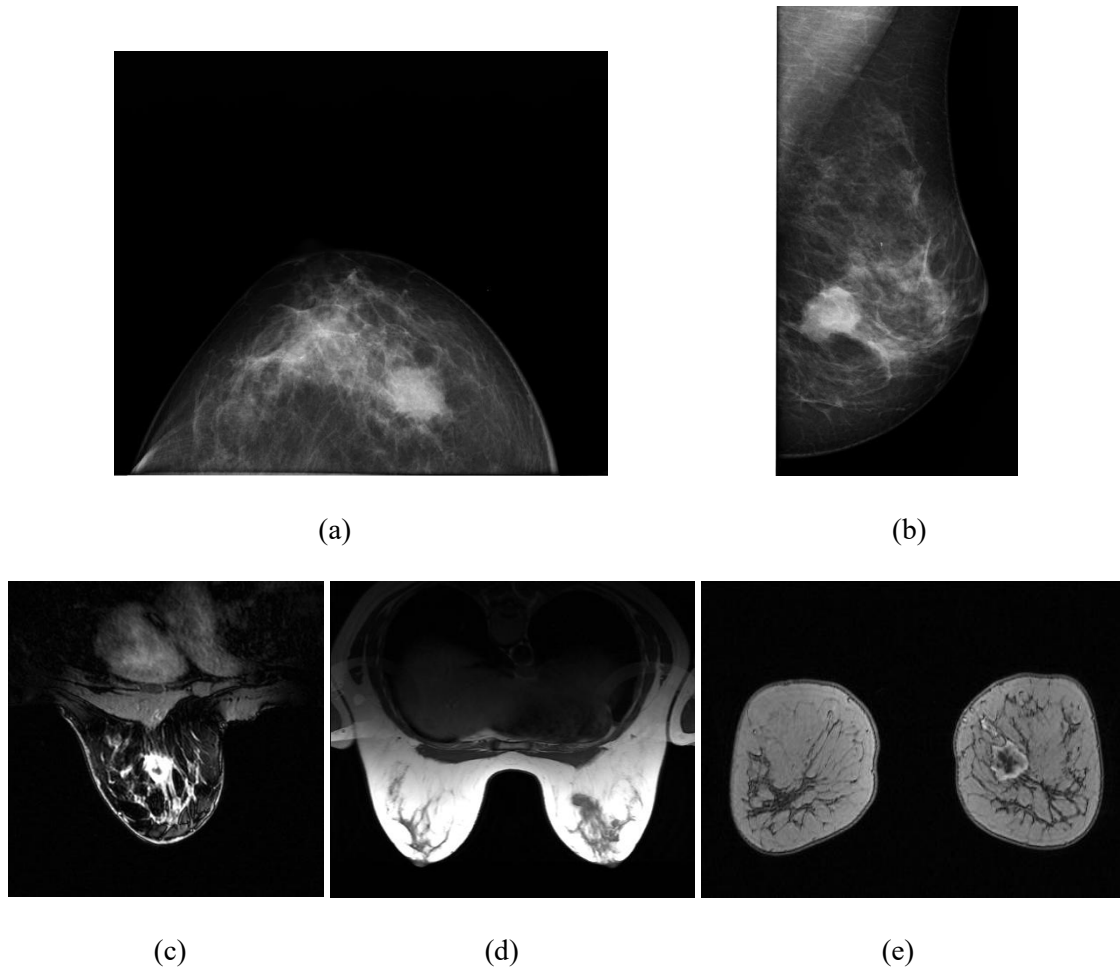(c)   (d)   (e)

Figure 1. Clinical images from the patient's left breast showing the presence of a tumor. Mammograms taken in two compression directions: (a) CC and (b) MLO. MR images in anatomical planes: (c) sagittal, (d) axial and (e) coronal.

A lesion of 2.5 x 2.2 x 2.5 cm^3 was measured in the left breast in CC, ML and AP (antero-posterior) directions, respectively. Images were saved to DICOM format and loaded into MIMICS 10.01 software (Materialise 2006). Segmentation of tumor from healthy tissues and image artifacts was performed semi-automatically, and a 3D geometric model of the breast was automatically built and saved in STL format (Standard Tessellation Language). The geometric model comprised two closed surfaces: one for the outer surface of the tumor and the other representing the skin breast. Figure 2 shows these surfaces and it can be observed that the surface representing the outer surface of the breast resulted in an irregular tessellation, pointing out the need of being refined. The outer surface of the breast was exported to ABAQUS software package (Simulia 2007) and re-meshed by means of an automated algorithm to obtain a regular mesh of linear triangular elements. Afterwards, a semi-automated meshing technique was employed to generate two 4-noded solid linear tetrahedral meshes: one filled the space enclosed by the outer surface of the tumor, and the other filled the space comprised between the surface of skin breast and the outer surface of the tumor, as can also be seen in Figure 2. Finally, tumor location was checked in the FE model by comparing its position with measurements carried out in the MR images. Table 1 summarizes the entities belonging to the FE model of the breast.

GEOMETRIC MODEL OF THE BREAST　　　　　**FINITE ELEMENT MESH**
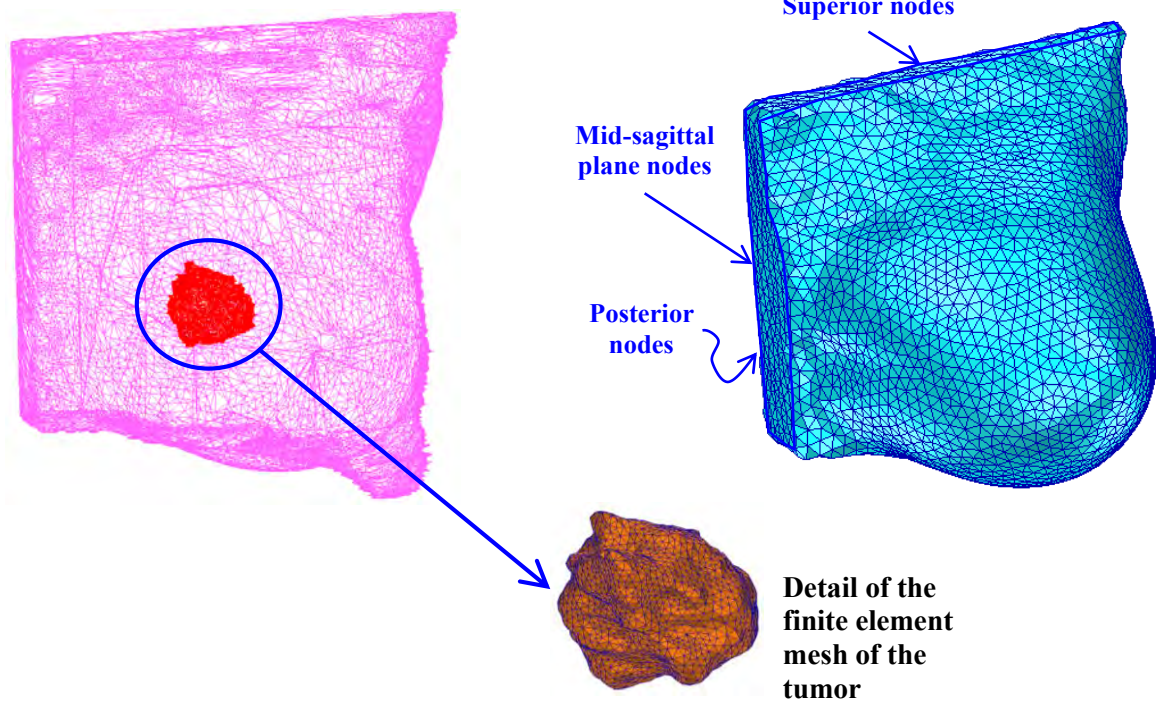

Figure 2. The tessellation of the surfaces obtained in MIMICS (Materialise 2006) (left) was smoothed in order to obtain a good quality mesh. On the right, the remeshing of the model by using linear triangular elements in the outermost surface of the breast. Nodes with fully restricted degrees of freedom are also indicated.

Table 1. Entities of the FE model of the breast.

MODEL REGION	FE ENTITY	NUMBER
Model	Nodes	9678
Internal tissues	Linear tetrahedrons	49291
	Nodes	5802
Tumor	Linear tetrahedrons	1934
	Nodes	769
Skin	Linear triangles	6210
	Nodes	3107

2.2. Constitutive modeling

Mechanical properties of breast tissues are highly dependent on factors such as age or physical condition (Lorenzen *et al* 2008). Also, in order to take into account the high deformability of the breast constitutive modeling of breast tissues has to be performed from the basis of finite elasticity (Fung 1999) (Holzapfel 2000).

The proposed model included four tissues: fat, gland, tumor and skin. Internal breast tissues (fat and gland) were assumed together as a homogenous media, as it was done in previous works (Pérez del Palomar *et al* 2008) (Lapuebla-Ferri *et al* 2011) (Roose *et al* 2005), and a constitutive neo-Hookean model was assumed for this *homogenized* tissue. The neo-Hookean model is used to characterize quasi-incompressible and hyperelastic media, such as the breast tissues. It uses the following strain-energy function:

$$\psi = c_1 \cdot (I_1 - 3)$$
(1)

where I_1 is the first invariant of the right Cauchy-Green deformation tensor and c_1 a constant that is equal to half the initial shear modulus μ of the tissue, which takes into account the rigidity of the breast.

Values previously reported by Samani and co-workers (Samani *et al* 2007) were used to compute the model constant c_1. In that work, mean values of elasticity moduli were computed from breast samples by using inverse analysis techniques ($E_{fat} \approx E_{gland}$ = 3.24 kPa) so an average value of E_{hom} = 3.24 kPa was assigned to the tetrahedrons of the FE model comprised between the outer surfaces of tumor and breast. Therefore, considering a Poisson's ratio of 0.49 a value of c_1= 0.54 kPa was obtained. Moreover, a parametric analysis was done to identify its relation with the accuracy of the results. On the other hand, a neo-Hookean model was also considered for the tumor. Since most breast tumors are several orders of magnitude stiffer than the surrounding tissue (Krouskop *et al* 1998) (O'Haggan and Samani 2008) a constant c_1 = 5.44 kPa corresponding to a tenfold E_{hom} and the same Poisson's ratio as the homogenized tissue was assigned to the finite elements representing the tumor. This value falls into the range of tumor stiffness stated by Samani *et al* (2007). Besides, skin mechanical properties also depend on the patient (Ulger *et al* 2003) so a hyperelastic model with a polynomial strain-energy density function Ψ_{sk} was assumed (Tong and Fung 1976):

$$\psi_{sk} = \sum_{i+j=1}^{N} c_{ij} \cdot (I_1 - 3)^i \cdot (I_2 - 3)^j$$
(2)

where I_1 and I_2 are the first and second invariants of the right Cauchy-Green tensor, respectively. In order to compute the constants c_{ij}, expression (2) was fitted for N=2 to the stress-strain experimental results obtained by Gambarotta *et al* (2005). By using the least-square method, the

following values were obtained: c_{10} = 31 Pa, c_{01} = 30 Pa, c_{11} = 22.5 Pa, c_{20} = 50 Pa and c_{02} = 60 Pa. These properties were assigned to the outermost triangular elements of the FE model with a uniform average thickness of 1 mm as reported in previous works (Han *et al* 2012) (Samani *et al* 2001) (Schnabel *et al* 2003) and assuming membrane behavior.

Constitutive relationships for the tissues were implemented in ABAQUS (Simulia 2007). Taking into account finite deformations and incompressibility of media, hybrid elements were considered to prevent excessive distortions.

2.3. Boundary conditions

Realistic boundary conditions were considered by observing the biomechanical behavior of the breast during mammography. As it is shown in Figure 2, displacements were fully restricted in the posterior nodes of the FE model. These nodes corresponded to the thoracic wall, which was assumed to be fixed. In addition, nodes located in the upper part and in the sagittal plane were also fully restricted by assuming that the body structures beyond this location do not interfere with breast deformation.

In order to simulate breast compressions in CC and MLO directions, two new meshes representing the compressing plates used in a mammography were included in the model (Figure 3). These plates were assumed to be rigid bodies compared to the breast tissues. In Figure 3 it can be seen that superior plate was modeled as a curved surface, and the inferior plate was modeled with its posterior part curved. This geometry assumption avoids convergence problems that arise when a sharp-edged rigid body contacts with a soft one.
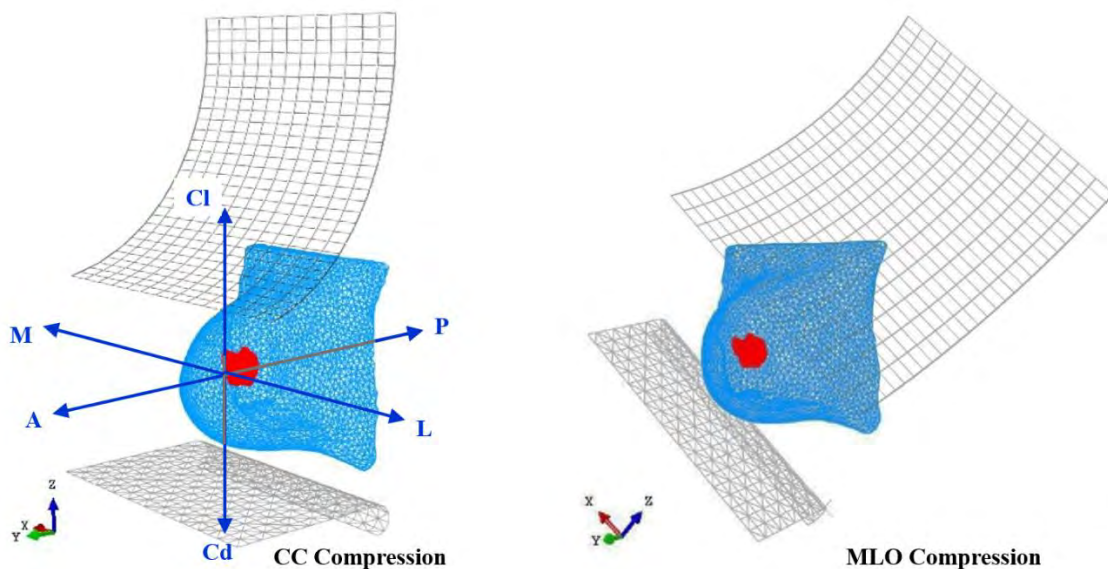

Figure 3. Non-rendered views of the FE breast model used to simulate mammographic compressions in the CC (left) and MLO (right) directions. Tumor is highlighted. Anatomical directions are also shown in the left views. A: anterior; P: posterior; Cl: cranial; Cd: caudal; L: lateral; M: medial.

Table 2 summarizes the features of the compressing plates in the FE model.

Table 2. FE entities of the compressing plates.

PLATE	NODES	ELEMENTS	SIZE (mm)
Superior	450	360	8.0 ± 1.70
Inferior	1035	972	5.5 ± 0.73

2.4. Simulation of breast compressions

Simulation steps of CC and MLO compressions were performed in ABAQUS (Simulia 2007) using the FE model following the reconstruction of the resonance magnetic images described before. Figure 4 illustrates how CC compression was simulated. Simulation of MLO compression followed a similar procedure, but the model was previously rotated 45º clockwise around an imaginary AP axis passing through the nipple and normal to the posterior surface of the model.

Each compression simulation comprised the following steps:

a) Gravity action was applied upwards to breast in AP direction in order to counteract breast deformation when MR images were obtained.
b) Lower plate was raised until it contacted the breast.
c) Gravity action was applied downwards until the breast rested on the inferior plate. Since then, the inferior plate remained fixed until the end of the simulation.
d) Superior plate was lowered until breast was highly compressed.

Coulomb's model was assumed to consider friction between the elements of the plates and the skin in contact during simulations. In such model, shearing stress developed in the interface varied linearly with the contact pressure between the two bodies. A constant friction coefficient $f_C = 0.1$ was assumed to relate both magnitudes, likewise in previous works (Chun *et al* 2012).

2.5. Tumor tracking methodology

The proposed methodology to track breast tumors is depicted in Figure 5. It consists of comparing the real mammograms of the patient obtained in CC and MLO directions with those computer-generated by means of FE simulations of mammographic compressions, which will be referred hereafter as *virtual mammograms*.

Virtual mammograms for each direction of compression were obtained by projecting the nodes of the deformed configuration of the model to the inferior compressing plate. From the resulting 2D point cloud, the nodes corresponding to the outermost contours of the breast and the tumor were isolated by means of an automated algorithm implemented in the software package MATLAB (The Mathworks 2013).
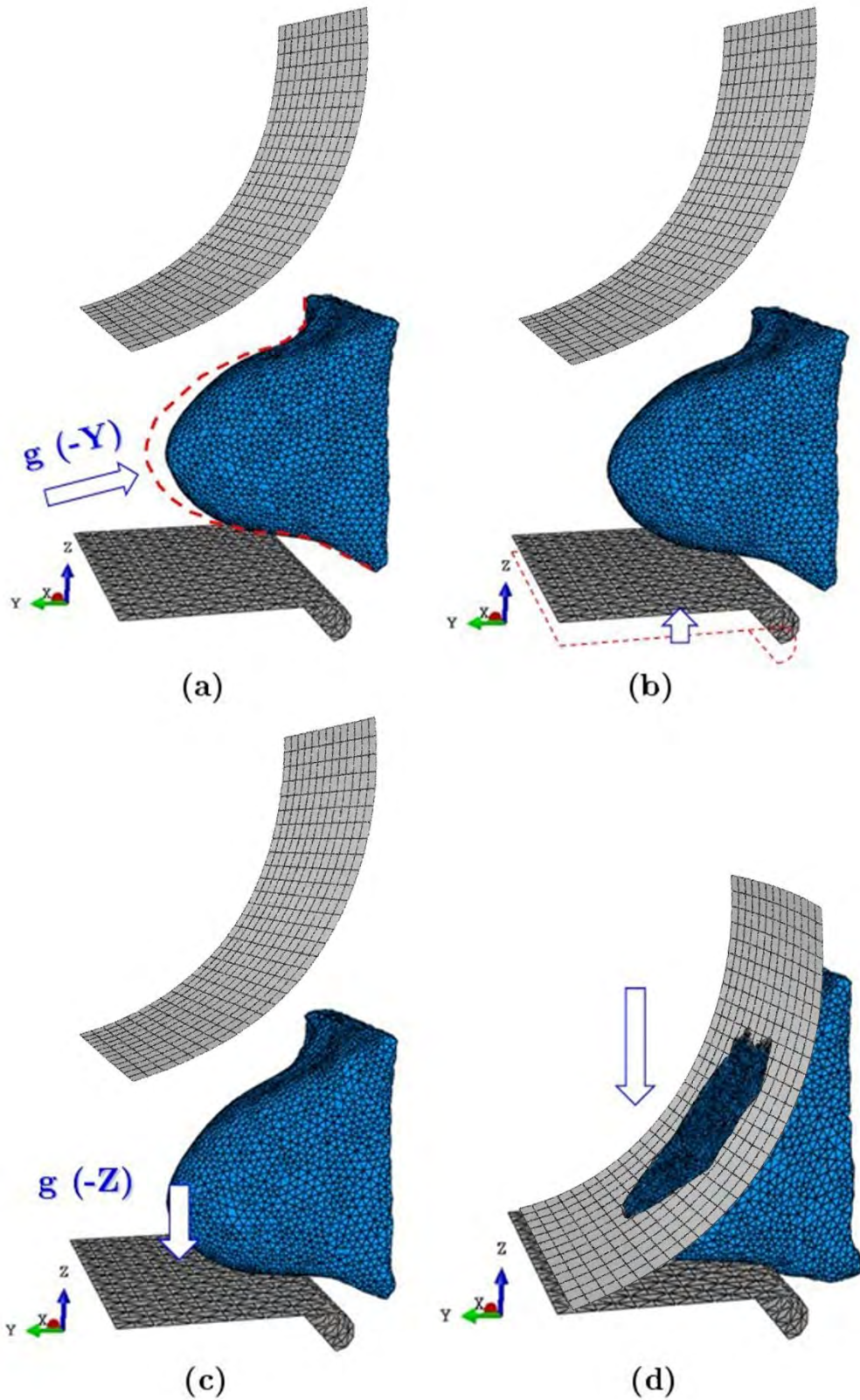
Figure 4. Steps of the simulation of mammographic compression in CC direction. (a) Gravity action applied to counteract breast deformation in MRI. (b) Lower plate is raised. (c) Gravity acting on the breast. (d) Upper plate descends to compress the breast.

PATIENT DATA

MR Images

Breast FE Model

SIMULATION

CC Compression

MLO Compression

Comparison

CC *Virtual* Mammogram

Image   Discretization

CC (Real) Mammogram

Comparison

Image   Discretization

MLO (Real)

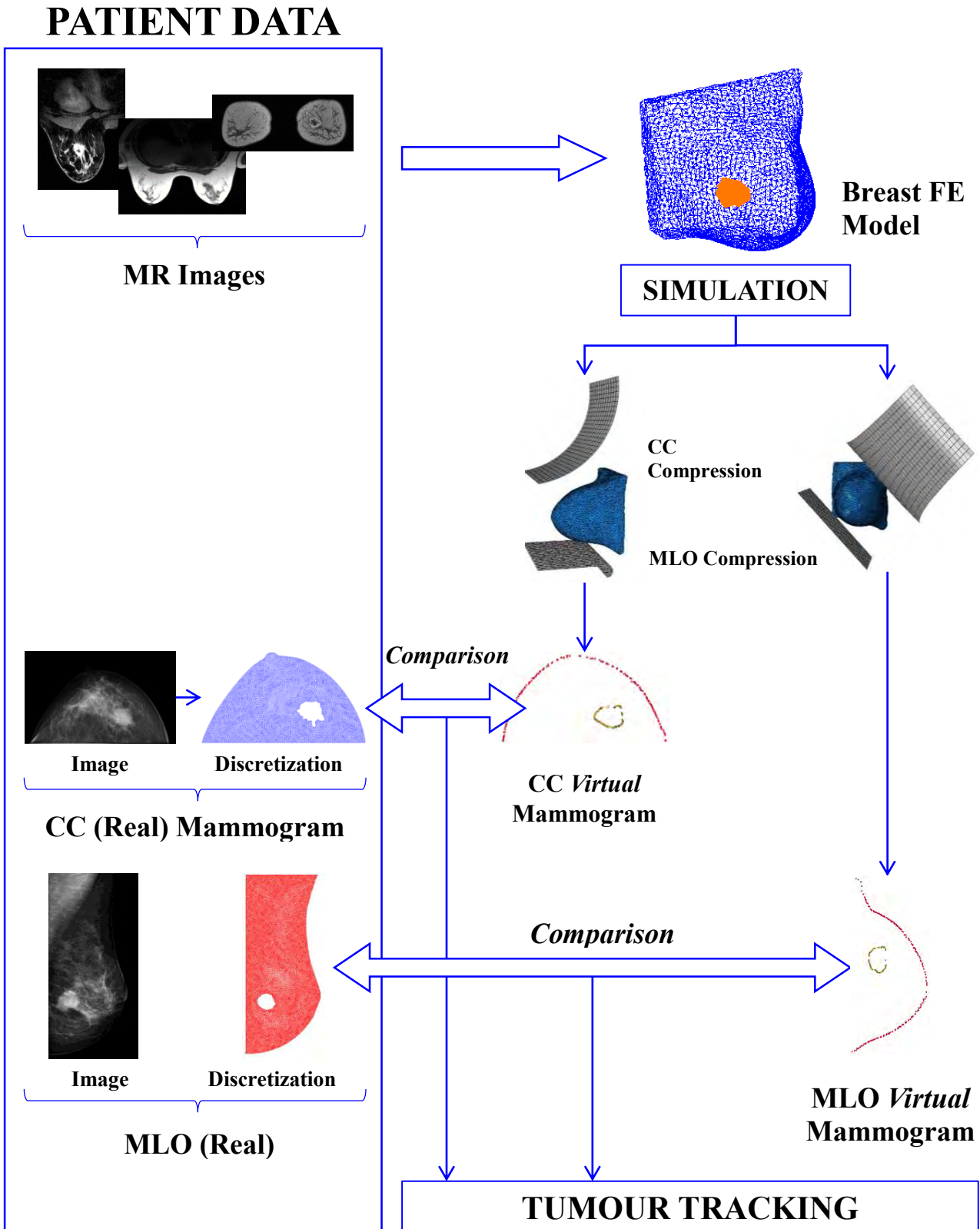MLO *Virtual* Mammogram

TUMOUR TRACKING

Figure 5. Scheme that shows the patient-based FE simulation methodology described in this work, from the numerical model construction to the tumour tracking. It is shown that *virtual mammograms* are generated from model compressions in CC and MLO directions and subsequently compared with the corresponding real mammograms.

Each real mammogram of the patient was discretized to compare it with the corresponding virtual mammogram and was turned into an in-plane tessellation, where only the nodes falling within the contours of the breast and the tumor were taken into consideration (Figure 6). Because of the mesh density, the contours could be considered as a continuous curve.
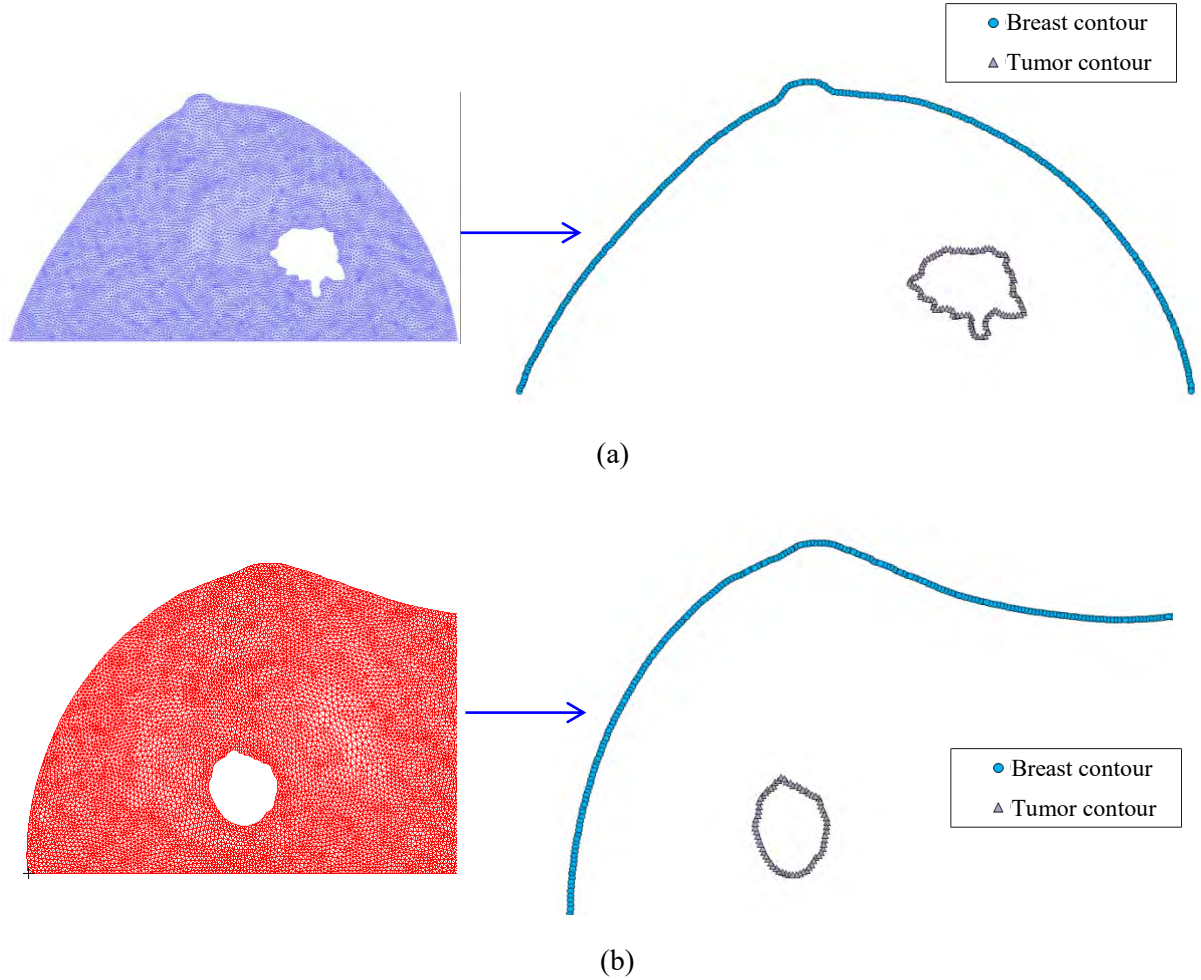

Figure 6. Discretization and contour extraction of the real mammograms of the patient depicted in Figure 1. (a) CC real mammogram. (b) MLO real mammogram.

For quantifying the similarity between real and virtual mammograms in each direction of compression, an automated algorithm based in the Golden Search Method (Yang *et al* 2005) was implemented in MATLAB. Two different planar regions were considered from the real and virtual mammogram contours (Figure 7): region Ω (blue) represented the real mammogram and region Ω' (grey) accounted for the virtual mammogram. Also, each region was composed by two contours: an open one representing the breast contour (Ω_b and Ω'_b) and a closed one representing the tumor contour (Ω_t and Ω'_t). Initially, regions Ω and Ω' were superimposed at a point n_p, which coincided with the projected position of the centroid of the nipple in the real and virtual mammograms. Hereafter, region Ω would remain fixed and region Ω' was subjected to a rotation angle $\theta \in \,] -\infty \, , +\infty \, [$ around the point n_p. Rotation angle θ take into account turning movement

exerted (voluntary or involuntarily) by the patient around a vertical axis during X-Ray mammography.

Proceeding in this way, a rigid transformation of the moving image contour was performed, and a new configuration $\Omega'(\theta)$ was acquired for each value of θ. Each point $i \in \Omega'_b(\theta)$ and $j \in \Omega'_t(\theta)$ was mapped to the closest points $k \in \Omega_b$ and $l \in \Omega_t$ in the breast and tumor contours, respectively, of the real mammogram.
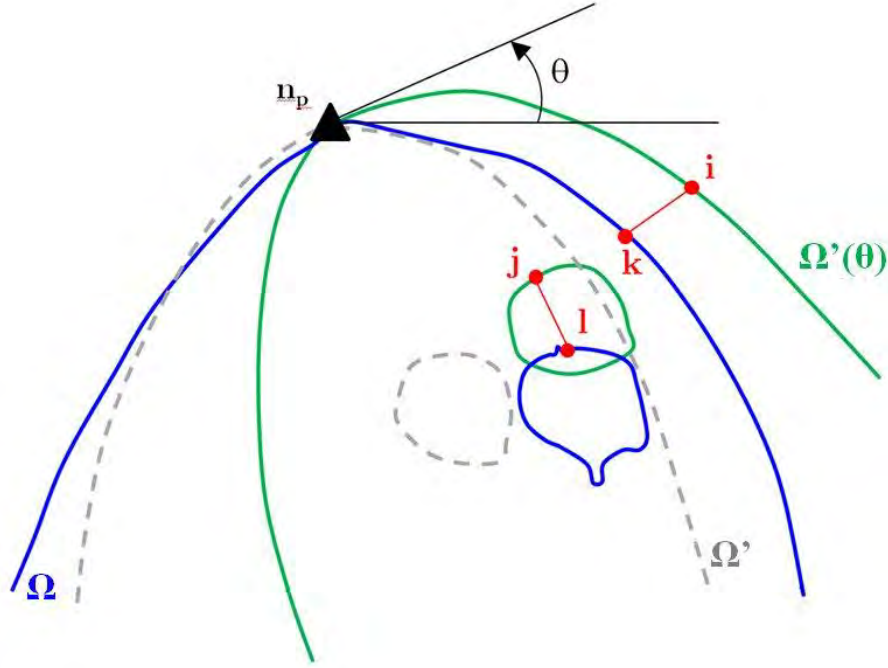

Figure 7. Comparison scheme of the contours of breast and tumor. Blue lines are the contours in the real mammogram. Virtual mammogram is represented in two colors: grey (initial orientation) and green (rotated).

Thus, the minimum difference between contours was obtained by solving an optimization problem by minimizing the value of a functional $F(\theta)$:

$$\min F(\theta) \rightarrow \begin{cases} \sum_{i=k=1}^{n} \left\| \Omega'_{b,i}(\theta) - \Omega_{b,k} \right\|^2 \\ \sum_{j=l=1}^{n} \left\| \Omega'_{t,j}(\theta) - \Omega_{t,l} \right\|^2 \end{cases} \tag{3}$$

being n the total number of points comprised into each contour in the region Ω. It was expected to find a single value of rotation angle θ – named optimum angle θ_p – capable to simultaneously satisfy expression (3), and so the best matching between breast and tumor contours would be achieved. Instead of this, two different values of θ_p were found for outer breast ($\theta_{p,b}$) and tumor contours ($\theta_{p,t}$). Finally, θ_p was computed as the average between $\theta_{p,b}$ and $\theta_{p,t}$. This will be properly discussed in Discussion section.

Assuming that a best matching situation exists, the following indicators were proposed:

- **BS$_{Av}$** *(Averaged Breast Similarity).* Accounted the averaged, percent similarity of breast contours (4).

$$BS_{Av}(\%) = \left(1 - \frac{\sum_{i=k=1}^{n}\left\|\Omega'_{b,i}(\theta_p) - \Omega_{b,k}\right\|}{\sum_{i=k=1}^{n}\left\|\Omega'_{b,i}(\theta_p) - \Omega_{b,k}\right\|_{\theta=0^{\circ}}}\right) \cdot 100 \tag{4}$$

- **TS$_{Av}$** *(Averaged Tumor Similarity)*. Accounted the averaged, percent similarity of tumor contours (5).

$$TS_{Av}(\%) = \left(1 - \frac{\sum_{j=l=1}^{n}\left\|\Omega'_{t,j}(\theta_p) - \Omega_{t,j}\right\|}{\sum_{j=l=1}^{n}\left\|\Omega'_{t,j}(\theta_p) - \Omega_{t,l}\right\|_{\theta=0^{\circ}}}\right) \cdot 100 \tag{5}$$

In equations (4) and (5), the term located in the numerator expressed the cumulative Euclidean distance between each point in a real contour and the closest one in the corresponding virtual contour for a given optimum angle θ_p. The resulting value is related to the expression in the denominator which computes the same distance prior to rotate the virtual mammogram (i. e., rotation angle $\theta = 0^{\circ}$).

On the other hand, a mesh convergence test was performed first to check the mesh density of the model and thus guarantee its suitability in the context of the proposed simulation methodology.

It should be considered that the proposed methodology was intended to involve the least number of parameters as possible in order to its future applicability in the clinical area. Thus, it is important to study the influence of the material parameters on the mechanical response of the model, especially its relevance over the indicators **BS$_{Av}$** and **TS$_{Av}$**. As the breast tissues have been considered as a single, homogenized media, the elastic constant to be taken into account are the neo-Hookean constant c_1 and the Poisson's ratio v. A parametrical study was carried out, and the results are depicted in the graphs of Figure 8. In that figure, it is shown that values of $c_1 \in [0.5 - 4]$ kPa and $v \in [0.45 - 0.49]$ were considered. These ranks of elastic constants are found in previous works involving breast simulations, and summaries of such values can be found in previous works (Pérez del Palomar *et al* 2008) (Tanner *et al* 2006). These results will be commented in Results section.
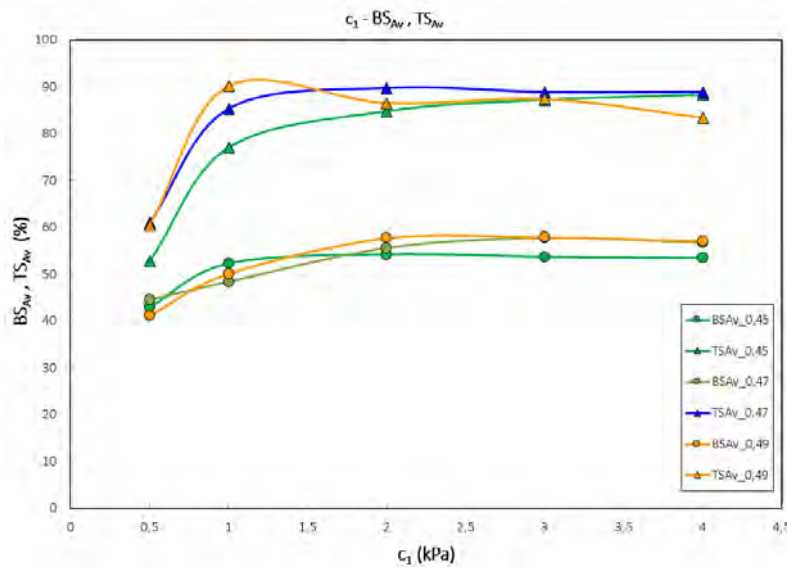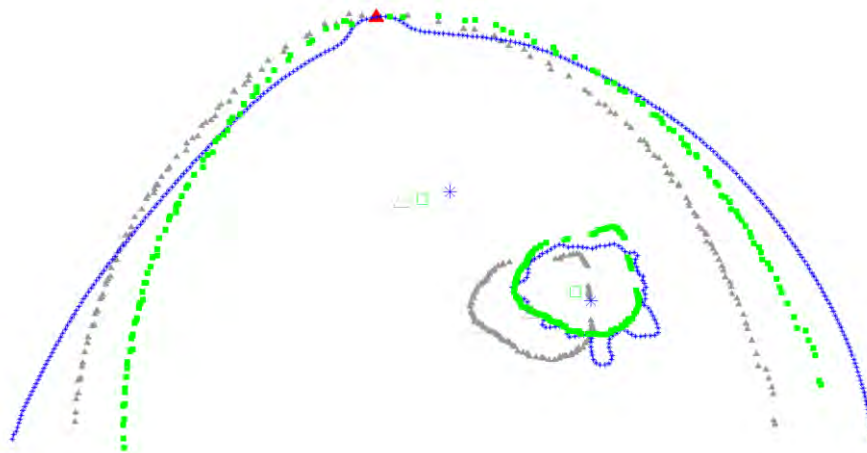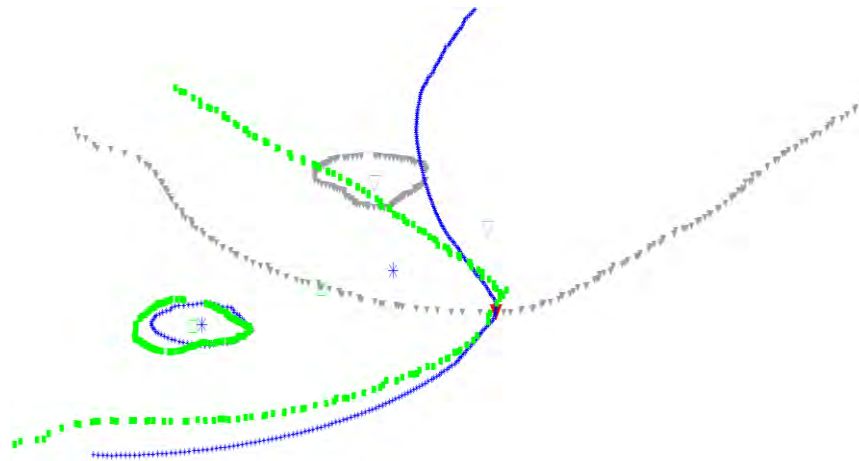

Figure 8. Relations between the neo-Hookean constant c_1 of the homogenized breast tissue and the proposed indicators **BS$_{Av}$** and **TS$_{Av}$**.

3. Results

Comparisons between contours of real and virtual mammograms for CC and MLO compressions are depicted in Figures 9a and 9b, respectively.

(a)

(b)

Figure 9. Superposition of real and virtual mammogram contours. (a) CC. (b) MLO. The centroid of each contour is remarked. Blue: contours of the real mammogram. Grey: contours of the virtual mammograms (initial position). Green: virtual mammogram position for the optimum angle θ_p.

From a qualitative point of view, contours of real and virtual mammograms showed a good similarity, especially in those concerning to CC compression. In Figure 9b, it is seen that the virtual MLO mammogram needs to be rotated 45º before performing a new rotation to find the optimum angle θ_p between virtual and real mammograms in this direction.

On another hand, three important results can also be noted by observing trends from Figure 8. First, it is noted the marked nonlinear relationship between the neo-Hookean constant and the proposed indicators BS_{Av} and TS_{Av}. Second, indicator BS_{Av} is higher than TS_{Av} throughout all the evaluated rank. This is probably influenced by the compression of the breast model that was reached throughout the simulation process. The degree of model compression D was evaluated

for the situation when the contours of virtual and real mammograms exhibited the maximum similitude (i. e., for $\theta_{p,av}$). The value of D was computed as the difference percentage of the average thickness of breast between the deformed and the undeformed configurations for each direction of compression, as can be seen of Table 3.

Table 3. Maximum values reached for the proposed indicators.

INDICATOR		CC	MLO
Optimum angle θ_p (deg)	Breast $\theta_{p,b}$	6	14.0
	Tumor $\theta_{p,t}$	8	13.0
Averaged $\theta_{p,av}$ (deg)		7	13.5
BS_{Av} (%)		63	66.2
TS_{Av} (%)		94	97.9
D (%)		38	28

The amount of breast compression for the patient's breast in this study is unknown, since force exerted during a mammographic compression is usually not recorded. Nevertheless, the compression values around the 30% are comprised within the values reported in previous works (Tanner *et al* 2016). Finally, the asymptotic trend of the curves of Figure 8 enforces the nonlinear nature of the problem. Considering these facts, and taking into account the uncertainties related to the mechanical constants of the tissues of the patient, constants c_I and ν were assumed as adjustment parameters in order to achieve a compression degree comparable to what is reached during a clinical setting and also to maximize the proposed indicators BS_{Av} and TS_{Av}. In fact, the optimum values shown in Table 3 were c_I = 1.98 kPa and ν = 0.485, and these are comprised within the ranks reported by Del Palomar *et al* (2008). When indicators BS_{Av} and TS_{Av} were maximized, the Euclidean distances between the centroids of the tumor and the breast contour between the real and the virtual mammograms – respectively, d_T and d_B – were measured for each direction of compression, as it can be seen in Table 4.

Table 4. Distances between centroids of the tumor (d_T) and the breast (d_M) contours measured between the real and virtual mammograms.

CENTROID DISTANCE (mm)	CC	MLO
d_T	3.84	2.41
d_B	4.91	12.20

The maximum value for d_T was lower than 4 mm in both directions of compressions. On the other hand, the values of d_B were higher, specially the measured in MLO compression, which was two-fold higher than the measured in CC compression. Once more, this is believed to be caused by the amount of compression of the breast model which is lower in MLO compression than in CC compression. It is interesting to note that even BS_{Av} shows a moderate value around 65%, the distance of between centroids of breast contour between both mammograms is significantly low. The presence of image artifacts – such the pectoral muscle – should also partly explain this difference.

In addition, the value of the friction coefficient f_c was kept constant to 0.1 during the simulations. This value is virtually impossible to know for every clinical setting. In previous works, in fact, friction between plates and skin is not accounted (Azar *et al* 2001) (Han *et al* 2012) or even taken into account with friction coefficient values that range from unspecified (Chung *et al* 2008) to low or moderate (Tanner *et al* 2006).

4. Discussion

A nonlinear mechanistic patient-specific FE model which reproduces the external features of a breast was built from MRI. Thus, it is assumed that a data set exist in the clinical scenario from which a FE model with a realistic geometry can be built. As an alternative to the medical images, other techniques can also be used – such as stereophotography (Khatam *et al* 2015) – but they are not usually found in the clinical practice because they are not used in breast diagnosis. It has to be taken into account that the authors did not participate in the taking of medical images from the patient, so some parameters that could have been properly measured during the process remained unknown, such as the angle of the plates relative to the breast, the amount of compression of breast patients, the force exerted to the breast, etc. As this is an obvious disadvantage, this kind of *blind* methodology obeys to the reality of clinical practice, in which image acquisition follows a different protocol than image analysis and thus the aforementioned parameters are not usually needed to be recorded. Nevertheless, the proposed methodology is intended to be as simple and straightforward as possible, and subsequently it uses the least number of parameters as possible. Besides, it is considered that a commercial simulation package – such the employed in the present framework – is more available to the physicians than an ad hoc software as used in another works (Solves-Llorens *et al* 2014).

A three-dimensional, FE model of the breast is complex because has to deal with three sources of nonlinearities: (1) geometrical, due to the large deformations arisen, (2) mechanical, due to the material models included and (3) the contact mechanics that appears when mammographic compressions are simulated. Regarding the first one, tetrahedral elements may not be adequate to support large deformations in a contact simulation, but they were chosen because their suitability to match a complex geometry such the breast is. Tetrahedrons also allow a rapid meshing of the model, which is interesting in order to a perform a quick surgery planning. Previous references of this kind of meshing to the breast – see for example Tanner *et al* (2011) – . The authors believe that a realistic geometry of a FE model is necessary in the context of this kind of methodology. Even previous works achieved good simulation results these are called into question since the model geometries were unrealistic (Mertzanidou *et al* 2014) (Solves-Llorens *et al* 2014).

Secondly, concerning mechanical properties, some simplifications were considered in this work to deal with constitutive modeling of breast tissues. Since the rigorous parametrization of breast material properties of the patient is not the aim of this work, internal arrangement of the breast tissues of the patient was not taken into account, so isotropy was assumed for all the internal breast tissues since they do not have a preferential fiber direction. As a consequence, a homogeneous and hyperelastic media was considered to englobe fat and gland. Besides, the homogeneity assumptions overlooked some uncertainties regarding the particular mechanical properties of the patient, since realistic mechanical properties of the tissues are difficult to be measured in a clinical situation. Average values from the literature were chosen for simplicity, as it was sustained from previous works (Samani *et al* 2000) (Lapuebla-Ferri *et al* 2011) and then assigned to some mechanical properties of breast internal. It was adopted the simplest non-linear constitutive model for the homogenized media, which is the neo-Hookean model, in which constant c_1 and Poisson's ratio ν were addressed as adjustment parameters. Besides, and for the sake of simplicity, the dependency of breast mechanical response with time was also neglected.

For example, viscoelastic behavior was not considered – unlike Hsu *et al* (2011) –. Finally, the contact problem implies the existence of contact pairs with a highly non-linear response. The authors believe that the contact nonlinearities involved in the simulations prevented the model to reach a higher compression degree, similar to that achieved during the clinical practice. There is little information about the contact mechanics which govern the interaction between skin and plates, so values of the friction coefficient were taken from literature in this work (Chung *et al* 2008). The geometry of the compressing plates was designed to be curved to allow the model to converge under a large compression.

The breast model was compressed in CC and MLO directions, as in a mammography. Virtual and real mammograms were compared by performing the following rigid transformations in-plane: superposition (translation) of the real and virtual mammogram in the node representing the nipple and rotation of one mammogram with respect to the other. This rotation accounted for patient rotations about her when in standing position. This was considered as the main reason why the two mammograms did not match. In the clinical practice of mammography, is difficult to prevent involuntary movements of the patient during the process. By means of this model, a mapping between the deformed shape of the breast during mammographic compression and the shape in MR imaging could found. When virtual mammograms were obtained, it was noted the anisotropic response of the breast at macro-scale stated by Ruiter and co-workers (Ruiter *et al* 2006). About the proposed indicators, the values of the angles $\theta_{p,b}$ and $\theta_{p,t}$ for the breast and the tumor were close enough to consider that the comparison method of both mammograms is adequate for each direction of compression. The low value of these angles indicated that the patient could rotate involuntarily during the clinical setting. According to these values, it can be assumed that there is a good matching especially between CC mammograms. The measured difference between centroids of the tumors is lower than 4 mm. By contrast, Mertzanidou *et al* (2014) accounted for a difference of around 11 mm mean with its intensity-based image registration framework. The authors postulate that the validity of this methodology is only achieved if a sufficient compression degree is reached, but its values are within the range of compressions reported in previous works (Samani *et al* 2001) (Ruiter *et al* 2006). In fact, in the latter work it was found a difference of 3.8 mm between real and simulated measurements in a similar work with a compression of 21%.

In this work, the stress-free reference configuration of the breast was not obtained. A stress-free configuration of the breast is not its natural state since biological tissues are subjected to stresses and strains *in vivo*. Moreover, MRI from which the model was built accounted for the breast to be highly deformed due to gravity. Although determining the stress-free reference configuration of the breast could lead to more reliable results (Rajagopal *et al* 2007), this practice is not easily implemented in a clinical setting. However, considering all the assumptions made in this work, it is possible to conceive a simulation framework without previously determine the breast reference state.

5. Conclusion

Human breast is a complex and heterogeneous organ composed of several soft tissues – mostly skin, gland and fat –. Biomechanically, breast has not a load-bearing function but it is able to withstand large deformations. On the other hand, X-ray-based mammography is a diagnostic and screening technique in which breast is highly compressed between two plates and radiated, thus obtaining and image called mammogram from which a suspicious mass can be easily detected. Besides, it is usual to employ other imaging techniques – such as MRI –to complement the initial diagnosis. Due to the high mobility of the breast, difficulties arise when a breast tumor must be tracked across images from the same of even different techniques. In fact, fusing

information from that variety of sources is a challenging task that can be facilitated by using computer simulations performed on numerical models. In this work, the authors propose a FE-based framework to help medical physicians to track breast tumors in-plane by using these image modalities.

The proposed simulation framework was intended to be implemented in a reasonable amount of time. Although some simplifications were considered in view of further translations into the clinical area, the obtained results were promising. Results indicate that it is possible to track in-plane a tumor with an error lesser than 5 mm by using exclusively rigid transformations, as was stated by Hipwell *et al* (2016). Deviation of the position estimate should be within 5 mm to be applicable for early breast diagnosis. Mapping of tumor tracking to tridimensional, physical space could be a future research step.

Finally, the proposed methodology is restricted to cases in which a suspicious mass is clearly defined against surrounding healthy tissue. In these cases, FE simulations provide a valuable insight into the biomechanical behavior of the subject involved, and, therefore, it can be come potentially useful to the clinicians. Nevertheless, future works in this direction requires of validation on a larger data set and a strategy to customize the model for each patient.

Acknowledgements

References

Azar FS, Metaxas DN, Schnall MD. A deformable finite element model of the breast for predicting mechanical deformations under external perturbations. Academic Radiology. 2001; 8: 965-75.

Chun HY, Jung HC, Kim MT, Kim KG, Ko KL. Needle insertion force exerted on various breast tissues: experimental study and finite element analysis. Biomedical Engineering Letters 2012; 2:173-78.

Chung JH, Rajagopal V, Nielsen PMF, Nash MP. A biomechanical model of mammographic compressions. Biomechanics and modelling in mechanobiology. 2008; 7:43-52.

Drukker K, Horsch K, Giger ML. Multimodality computerized diagnosis of breast lesions using mammography and sonography. Academic Radiology. 2005; 12: 970-79.

Fung, Y. Biomechanics: mechanical properties of living tissues. New York, USA: Springer-Verlag, 1999.

Gambarotta L, Massabò R, Morbiducci R, Raposio E, Santi P. In vivo experimental testing and model identification of human scalp skin. Journal of Biomechanics 2005; 38:2237-47.

Guo Y, Sivaramakrishna R, Lu CC, Suri JS, Laxminarayan S. Breast image registration techniques: a survey. Medical and Biological Engineering and Computing. 2006; 44: 15-26.

Han L, Hipwell JH, Tanner C, Taylor Z, Mertzanidou T, Cardoso J, Ourselin S, Hawkes DJ. Development of patient-specific biomechanical models for predicting large breast deformation. Physics in Medicine and Biology 2012; 57:455-72.

Han L, Hipwell J, Eiben B, Barratt D, Modat M, Ourselin S, Hawkes DJ. A nonlinear biomechanical model based registration method for aligning prone and supine MR breast images. IEEE Transactions on Medical Imaging. 2014; 33:682-94.

Hipwell JH, Vavourakis V, Han L, Mertzanidou T, Eiben B, Hawkes DJ. A review of biomechanically informed breast image registration. Physics in Medicine & Biology. 2016; 61:R1-R31.

Holzapfel, GA. Nonlinear solid mechanics: a continuum approach for engineering. Chichester, England: Wiley, 2000.

Hopp T, Dietzel M, Baltzer P, Kreisel P, Kaiser W, Gemmeke H, Ruiter N. Automatic multimodal 2D/3D breast image registration using biomechanical FE models and intensity-based optimization. Medical Image Analysis 2013; 17: 209-18.

Hsu CML, Palmeri ML, Segars WP, Veress AI, Dobbins III JT. An analysis of the mechanical parameters used for finite element compression of a high-resolution 3D breast phantom. Medical Physics. 2011; 38:5756-70.

Jemal A, Center MM, DeSantis C, Ward E. Global patterns of cancer incidence and mortality rates and trends. Cancer Epidemiology, Biomarkers & Prevention 2010; 19:1077-95.

Khatam H, Reece GP, Fingeret MC, Markey MK, Ravi-Chandar K. In-vivo quantification of human breast deformation associated with the position change from supine to upright. Medical Engineering & Physics 2015; 37:13-22.

Krouskop TA, Wheeler TM, Kallel F, Garra BS, Hall T. Elastic moduli of breast and prostate tissues under compression. Ultrasonic Imaging 1998; 20:260-74.

Kuhlmann M, Fear EC, Ramirez-Serrano A, Federico S. Mechanical model of the breast for the prediction of deformation during imaging. Medical Engineering & Physics. 2013; 35:470-8.

Lapuebla-Ferri A, Pérez del Palomar A, Herrero J, Jiménez-Mocholí AJ. A patient-specific FE-based methodology to simulate prosthesis insertion during an augmentation mammoplasty. Medical Engineering & Physics 2011; 33:1094-102.

Lee A, Rajagopal V, Doyle A, Nielsen PM, Nash M. Breast lesion co-localisation between X-Ray and MR images using finite element modelling. Medical Image Analysis 2013; 17: 1256-64.

Lorenzen J, Sinkus R, Biesterfeldt M, Adam G. Menstrual-cycle dependence of breast parenchyma elasticity: estimation with magnetic resonance elastography of breast tissue during the menstrual cycle. Investigative Radiology 2003; 38:236-40.

Malur S, Wurdinger S, Moritz A, Michels W, Scheneider A. Comparison of written reports of mammography, sonography and magnetic resonance mammography for preoperative evaluation of breast lesions, with special emphasis on magnetic resonance imaging. Breast Cancer Research 2001; 3:55-60.

Materialise. MIMICS 10.01 User Documentation. Leuven, Belgium: Materialise, 2006.

Mertzanidou T, Hipwell J, Johnsen S, Han L, Eiben B, Taylor Z, Ourselin S, Huisman H, Mann R, Bich U, Karssemeijer N, Hawkes D. MRI to X-ray mammography intensity-based registration

with simultaneous optimisation of pose and biomechanical transformation parameters. Medical Image Analysis 2014; 18:674-83.

O'Hagan JJ, Samani A. Measurement of the hyperelastic properties of tissue slices with tumour inclusion. Physics in Medicine and Biology 2008; 53:7087-106.

Ong RE, Ou JJ, Miga MI. Non-rigid registration of breast surfaces using the Laplace and diffusion equations. BioMedical Engineering OnLine 2010; 9:8.

Pathmanathan P, Gavaghan DJ, Whiteley JP, Chapman SJ, Brady JM. Predictiong tumor lacation by modelling the deformation of the breast. IEEE Transactions on Biomedical Engineering 2008; 55:2471-80.

Pérez del Palomar A, Calvo, B, Herrero J, López J, Doblaré M. A finite element model to accurately predict real deformations o the breast. Medical Engineering & Physics 2008; 30:1089-97.

Rajagopal V, Chung JH, Bullivant D, Nielsen PMF, Nash MP. Determining the finite elasticity reference state from a loaded configuration. International Journal for Numerical Methods in Engineering 2007; 72:1434-51.

Rajagopal V, Lee A, Chung JH, Warren R, Highnam RP, Nash MP, Nielsen PMF. Creating individual-specific biomechanical models of the breast for medical image analysis. Academic Radiology 2008; 15:1425-36.

Roose L, De Maerteleire W, Mollemans W, Suetens P. Validation of different soft tissue simulation methods for breast augmentation. International Congress Series 2005; 1281:485-90.

Ruiter NV, Stotzka R, Müller TO, Gemmeke H, Reichenbach JR, Kaiser WA. Model-based registration of X-ray mammograms and MR images of the female breast. IEEE Transactions on Nuclear Science 2006; 53:204-11.

Samani A, Bishop J, Ramsay E, Plewes DB. Breast tissue deformation finite element modelling for MRI/X-ray mammography data fusion. Proceedings of the International Workshop on Digital Mammography. Toronto, ON, Canada, 2000; 763-69.

Samani A, Bishop J, Yaffe MJ, Plewes DB. Biomechanical 3-D finite element modelling of the human breast using MRI data. IEEE Transactions on Medical Imaging 2001; 20:271-79.

Samani A, Zubovits J, Plewes D. Elastic moduli of normal and pathological human breast tissues: an inversion-technique-based investigation of 169 samples. Physics in Medicine and Biology 2007; 52:1565-76.

Schnabel JA, Tanner C, Castellano-Smith AD, Degenhard A, Leach MO, Hose DR, Hill DLG, Hawkes DJ. Validation of nonrigid image registration using finite-element methods: application to breast MR images. IEEE Transactions on Medical Imaging 2003; 22:238-47.

Simulia, Inc. ABAQUS/standard version 6.11. Pawtucket, RI, USA, 2007.

Solves-Llorens JA, Rupérez MJ, Monserrat C, Feliu E, García M, Lloret M. A complete software application for automatic registration of x-ray mammography and magnetic resonance images. Medical Physics 41, 081903 (2014); doi: 10.1118/1.4885957.

Tanner C, Schnabel JA, Hill DLG, Hawkes DJ. Factors influencing the accuracy of biomechanical breast models. Medical Physics. 2006; 33:1758-69.

Tanner C, White M, Guarino S, Hall-Craggs MA, Douek M, Hawkes DJ. Large breast compressions: observations and evaluation of simulations. Medical Physics. 2011; 38:682-90.

The Mathworks, Inc. 2013. MATLAB 2013b user's manual. Natick, MA, USA.

Tong P, Fung Y. The stress-strain relationship for the skin. Journal of biomechanics 1976; 9:649-57.

Ulger H, Erdogan N, Kumanlioglu S, Unur E. Effect of age, breast size, menopausal and hormonal status on mammographic skin thickness. Skin Research and Technology 2003; 9:284-89.

Yang WY, Cao W, Chung TS, Morris J. Applied Numerical Methods using MATLAB. 2005. John Wiley and Sons, Inc. Hoboken, NJ, USA.